Vibrational Analysis of Peptides, Polypeptides, and Proteins. V. Normal Vibrations of β-Turns

S. KRIMM and JAGDEESH BANDEKAR, *Biophysics Research Division and Department of Physics, The University of Michigan, Ann Arbor, Michigan 48109*

Synopsis

The normal modes have been calculated for β-turns of types I, II, III, I′, II′, and III′. The complete set of frequencies is given for the first three structures; only the amide I, II, and III modes are given for the latter three structures. Calculations have been done for structures with standard dihedral angles, as well as for structures whose dihedral angles differ from these by amounts found in protein structures. The force field was that refined in our previous work on polypeptides. Transition dipole coupling was included, and is crucial to predicting frequency splittings in the amide I and amide II modes. The results show that in the amide I region, β-turn frequencies can overlap with those of the α-helix and β-sheet structures, and therefore caution must be exercised in the interpretation of protein bands in this region. The amide III modes of β-turns are predicted at significantly higher frequencies than those of α-helix and β-sheet structures, and this region therefore provides the best possibility of identifying β-turn structures. Amide V frequencies of β-turns may also be distinctive for such structures.

INTRODUCTION

The region in which a polypeptide chain reverses its direction by ~180° is often referred to as a β-turn. Such regions, consisting of the three peptide groups at the turn, comprise a significant component of globular proteins: in a recent analysis[1] we found that in 38 nonhomologous proteins, 29% of the amino acids occur in β-turns.

Specific conformations for such β-turns were first characterized in detail by Venkatachalam[2] on the basis of stereochemical criteria, although analogous structures were also proposed at this time from a study of the "cross-β" conformation of fibrous proteins.[3] Three main types of β-turns were described,[2] all having an internal hydrogen bond between the CO group of residue 1 and the NH group of residue 4. Types I and II are nonhelical conformations, whereas type III corresponds to one turn of a 3_{10}-helix. The standard form of the type II turn requires a glycine residue at the 3-position, there being no such restrictions for the other turns. Structures which have mirror-image arrangements of the backbone atoms were also found to be possible,[2] and are designated as types I′, II′, and III′.

A subsequent analysis of eight protein structures[4] revealed that five additional types of turns could exist, designated IV, V, V′, VI, and VII.

Biopolymers, Vol. 19, 1–29 (1980)

0006-3525/80/0019-0001$01.00

Type IV comprises any of the β-turns of types I–III′ in which the values of two or more angles ϕ and ψ at residues 2 and 3 differ by at least 40° from the typical angles for these types. A type V turn corresponds to a seven-membered hydrogen-bonded ring conformation (compared to a 10-membered ring for the others). The type VI turn has a *cis* proline at the 3-position. In the type VII turn the distance between the C^{α} atoms of residues 1 and 4 is less than 7 Å, a minimal criterion required of all β-turns, but instead of a reversal in direction there is a "kink" in the chain. A later detailed analysis of 29 protein structures[5] revealed that all of the above types of β-turns occur: type I is the most frequent (42% of the total of 421 observed), followed by types III (18%), II (15%), and IV (8%). Mirror-image types are less frequent: type I′ had a frequency of 3%, type II′ a frequency of about 5%, and type III′ a frequency of 3%. The other types were found rarely. It should be noted that in this study,[5] β-turns were considered "ideal" if any of the ϕ and ψ at residues 2 and 3 did not differ by more than 50° from the values typical for that type. With this definition not even all ideal β-turns had an internal hydrogen bond, whereas some nonideal turns did have such a bond.

In view of their significant contribution to the structure of proteins, it is important that physical methods be available to identify and characterize β-turns. Vibrational spectroscopic techniques, namely ir and Raman, can be useful for this purpose. Although experimental studies on model compounds[6,7] can suggest the existence of such conformations, it is essential to be able to predict the vibrational frequencies of β-turns in order to have a sound theoretical basis for assigning characteristic bands to such structures. We have, therefore, calculated the normal vibration frequencies of several types of β-turns. A preliminary report of the results has been given[1]; we present here the details of the calculations.

NORMAL VIBRATION CALCULATIONS

There are two main problems associated with the calculation of the normal modes of vibration of β-turns: the large variability in the angles $(\phi,\psi)_2$ and $(\phi,\psi)_3$ found for any particular type of turn,[5] and the large variety of side-chain residues associated with these positions.[5] We have chosen to deal with the first problem by computing the frequencies associated with β-turns having "standard" angles[2,4,5] and then computing the effects on the frequencies of variations from the standard structures. In this way it is possible to develop some feeling for the importance that variations in different parts of the structure have in shifting the frequencies. We have not dealt with the second problem in any detail at this stage, using an alanyl residue for all side chains (except in type II, where a glycyl residue was used in the 3-position; variations with alanyl at this position will be discussed later). This is probably not too bad an approximation, since initially we will be most interested in the characteristic modes associated with the peptide group and with the backbone, and these are not likely to be strongly affected by the side-chain structure beyond the C^{β}-position.

The system chosen to represent a type I β-turn is CH_3-CO-$(Ala)_4$-NH-CH_3, and it is shown schematically in Fig. 1. An isolated β-turn can be adequately described by two sets of dihedral angles, namely $(\phi,\psi)_2$ and $(\phi,\psi)_3$, and it might be thought, therefore, that the model system CH_3-CO-$(Ala)_2$-NH-CH_3 would suffice to calculate the normal modes of β-turns in proteins. In fact, a calculation for such a structure showed that this was not the case. The β-turns in proteins have peptide groups adjoining the three of the tripeptide system, and transition dipole coupling[8,9] between these groups is significantly different for the case of three as compared to five groups. We have therefore selected the larger model as more representative of β-turns in proteins. (Conversely, it should be kept in mind that the frequencies calculated here will not necessarily be applicable to small peptide β-turns having fewer than five peptide groups.)

The bond lengths and angles used in these calculations were the same as in our previous work.[10–12] The dihedral angles at residues 1 and 4 were maintained, in the standard β-turn types I–III, at values consistent with the continuation of the chains in an antiparallel-chain pleated-sheet structure, viz., $(\phi,\psi)_1 = (\phi,\psi)_4 = -139°, 135°$. For β-turn types I′–III′, these values of ϕ,ψ were sterically disallowed, and we therefore used $(\phi,\psi)_1 = (\phi,\psi)_4 = -60°, 120°$. We computed the complete normal mode spectrum of β-turn types I–III (and their mirror-image conformations), and for these we took the typical dihedral angles[2] as: I—$(\phi,\psi)_2 = -60°, -30°$, $(\phi,\psi)_3 = -90°, 0°$; II—$(\phi,\psi)_2 = -60°, 120°$, $(\phi,\psi)_3 = 80°, 0°$; III—$(\phi,\psi)_2 = -60°, -30°$, $(\phi,\psi)_3 = -60°, -30°$ (and the negative of these values for I′–III′).

In the standard structures, internal hydrogen bonds were formed, viz.,

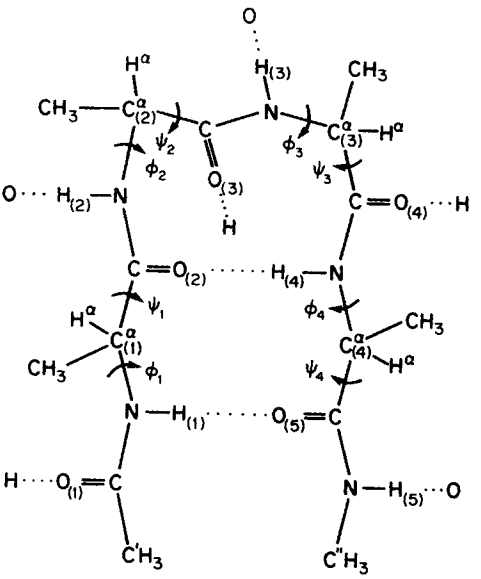

Fig. 1. Schematic illustration of a β-turn of CH_3-CO-$(Ala)_4$-NH-CH_3 with external hydrogen bonds included.

$H_{(1)}\cdots O_{(5)}$ and $H_{(4)}\cdots O_{(2)}$. When structural variations were examined these distances changed, and in some cases, these bonds were no longer present. In order to take account of this effect, we allowed the hydrogen-bond force constant, $f(H\cdots O)$, to decrease linearly from its value[10] of 0.125 md $Å^{-1}$ at $r(H\cdots O) = 1.8$ Å to zero at $r(H\cdots O) = 5.0$ Å. [Although the hydrogen bond might be considered to be absent for $r(H\cdots O) \geq 2.5$ Å,[5] the above variation still allows for some nonbonded interactions at longer distances.] For the external CO and NH groups, the presence or absence of hydrogen bonds has a significant effect on the amide II and III frequencies (lowering them when external hydrogen bonds are not included[1]). Since these groups would usually be expected to be hydrogen bonded in proteins, we have incorporated the effects of such bonding by placing a hydrogen atom in the appropriate position with respect to the CO group and an oxygen atom in a comparable position with respect to the NH group (Fig. 1). These atoms, and $f(H\cdots O) = 0.125$ md $Å^{-1}$, were included in the computations and were kept constant during variations in dihedral angles. Although such values may not exactly match those found in particular proteins, their inclusion should provide a valid measure of the influence of hydrogen bonding on the above amide frequencies. (It should be noted that such hydrogen bonds would not be expected for oligopeptides in nonpolar solvents, and the effects on amide II and III indicated by our earlier calculations[1] would be expected to prevail.)

The force field for the calculations was taken from our previous work on polypeptide structures.[10-12] The effects of transition dipole coupling[8,9] were incorporated only for the amide I and II modes. In the amide III mode, coordinates other than NH in-plane bending make a significant contribution, and as in the case of β-poly(L-alanine),[11] the coupling of NH in-plane bending modes does not have an appreciable effect in perturbing the frequencies. (This is in contrast to the case of polyglycine I,[10] in which NH in-plane bending makes comparable contributions to the amide II and III modes.) The positions and orientations of the transition dipole moments with respect to the CO and NH bonds were assumed to be the same as in previous work,[10,11] and all interactions were included. We do not, however, have independent information on the magnitudes of the effective moments, $\Delta\mu_{\text{eff}}$, in the β-turn as compared with the β-sheet and α-helix structures. We have, therefore, computed the amide I and II frequencies for a range of values of this parameter: $\Delta\mu_{\text{eff}} = 0$, 0.30, 0.35, and 0.45 D for amide I [for β-poly(L-alanine) we found[11] that $\Delta\mu_{\text{eff}} = 0.37$ D], and $\Delta\mu_{\text{eff}} = 0$, 0.20, 0.27, and 0.40 D for amide II [the value found for β-poly(L-alanine) was $\Delta\mu_{\text{eff}} = 0.27$ D].

In the calculations for the structures whose dihedral angles varied from the standard values, we attempted to choose dihedral angles representative of those found in proteins. Our analysis of the structural data on 38 nonhomologous proteins in the Brookhaven National Laboratory Protein Data Bank indicated that the majority of β-turns of types I and II had average variations in ϕ_2 of up to $-30°$, in ψ_2 and ϕ_3 of up to $\pm 30°$, and in ψ_3 of up

to ±35°. For type III β-turns the comparable values were: ϕ_1 up to −10°, ψ_2 up to −25°, ϕ_3 up to +15° and −25°, and ψ_3 up to +15° and −20°. We therefore computed the normal vibration frequencies of such β-turns with each angle varied from the standard value by the above amounts. Since, as indicated above, transition dipole coupling also involves peptide groups 1 and 5, it was desirable to investigate the effects of variations in $(\varphi,\psi)_1$ and $(\phi,\psi)_4$ on the characteristic β-turn frequencies. Examination of the protein data led us to select for normal mode calculations the following additional values of these dihedral angles: $\phi_1 = -60°, 120°$; $\psi_1 = -60°, -120°$; $\phi_4 = -60°, 120°$; and $\psi_4 = -60°, -120°$ for types I and II β-turns; and $\phi_1 = -60°$; $\psi_1 = 40°, -40°$; $\phi_4 = -80°, -45°$; and $\psi_4 = 60°, -40°$ for type III β-turns. In these computations external hydrogen bonds remained constant and internal hydrogen bonds varied according to the algorithm discussed above.

In the above calculations the force field was assumed to remain constant when the structure was varied. Frequency shifts therefore arise from changes in mechanical coupling (G matrix elements) and from variations in transition dipole coupling. This may not, of course, actually be the case. Force constants may also change with structure, and there is some evidence for such changes in going from β-poly(L-alanine) to α-poly(L-alanine).[12] While some of these changes may be associated with differences in hydrogen-bond strength between these structures, others may be inherently related to the dependence of force constants on internal structure. There is no detailed information available at the present time that would permit this factor to be taken into account in the calculation, and we have therefore proceeded on the (nevertheless reasonable) assumption that the main influence on the frequencies arises from structural differences. There is much evidence for the validity of this concept, an example of which is the rotational isomers of chlorinated hydrocarbons.[13]

RESULTS

We present in Tables I–III the calculated frequencies for standard β-turns of types I–III, respectively, in the absence of transition dipole coupling. The frequencies for NH stretch, CH_3 asymmetric stretch, CH_3 symmetric stretch, $C^\alpha H^\alpha$ stretch, CH_3 asymmetric bend, and CH_3 symmetric bend are not given explicitly, since they are not particularly distinctive; only the frequency intervals and numbers of normal modes are given. For the other frequencies, all contributions to the potential energy equal to or greater than 10% are included. The internal coordinates correspond to the structure in Fig. 1 and are the same as those used in our previous studies.[10–12] The C and N atoms of the peptide groups are numbered the same as the labeled O and H atoms of these groups in Fig. 1. The H^α atoms, and the CH_3 groups attached to the C^α atoms, have the same number as the corresponding C^α atoms.

As developed in our earlier work,[8–12] the observed splittings in the amide

TABLE I
Calculated Frequencies of a Type I β-Turn of CH_3-CO-$(Ala)_4$-NH-CH_3

Frequency (cm^1)	Potential Energy Distribution[a]
3275–3265	NH str: 5 modes
2979–2976	CH_3 asym str: 12 modes
2942–2941	CH_3 sym str: 6 modes
2876–2873	$C^\alpha H^\alpha$ str: 4 modes
1676	C=O(5) str(68), CN(5) str(13)
1673	C=O(2) str(51), C=O(1) str(22)
1671	C=O(1) str(49), C=O(2) str(23)
1666	C=O(3) str(56), C=O(4) str(20)
1665	C=O(4) str(55), C=O(3) str(21)
1579	NH(5) ipb(53), $C''H_3$ sym bend(22)
1569	NH(4) ipb(49), CN(4) str(23)
1567	NH(1) ipb(43), CN(1) str(20)
1554	NH(2) ipb(51), CN(2) str(23)
1540	NH(3) ipb(47), CN(3) str(29)
1468–1451	CH_3 asym bend: 12 modes
1380–1374	CH_3 sym bend: 6 modes
1371	H^α(1) bend 1(41), $C'H_3$ sym bend(14)
1371	H^α(3) bend 1(22), H^α(4) bend 1(19)
1356	H^α(3) bend 1(28), H^α(4) bend 1(27)
1353	H^α(2) bend 1(58), CH_3(1) sym bend(11)
1331	NH(1) ipb(28), C'C str(18), CN(1) str(16), C=O(1) ipb(13)
1324	NH(4) ipb(23), C^α(3)C str(15), CN(4) str(15), H^α(3) bend 1(11)
1305	NH(3) ipb(29), C^α(2)C str(15), CN(3) str(10)
1299	NH(2) ipb(28), C^α(1)C str(11), NH(3) ipb(11), CN(2) str(10), H^α(1) bend 1(10)
1293	NH(5) ipb(37), C^α(4)C str(17), H^α(4) bend 1(13), CN(5) str(12), C=O(5) ipb(10)
1212	NC^α(2) str(30), NC^α(1) str(22)
1199	NC^α(3) str(31), NC^α(4) str(11)
1189	NC^α(4) str(30), NC^α(3) str(14), C^α(3)C str(10), CH_3(3) rock 2(10)
1166	NC^α(1) str(25), NC^α(2) str(14)
1116	NC'' str(19), C^α(4)C^β str(14)
1113	CH_3(3) rock 1(18), $C''H_3$ rock 2(16), C^α(4)C^β str(10)
1111	$C'H_3$ rock 1(32), $C'H_3$ rock 2(11), C^α(1)C^β str(10)
1106	$C''H_3$ rock 2(29), CH_3(3) rock 1(18), $C''H_3$ rock 1(11), C^α(4)C^β str(10)
1102	CH_3(2) rock 1(20), C^α(3)C^β str(13)
1095	CH_3(1) rock 1(20), CH_3(2) rock 1(17), C^α(2)C^β str(17)
1091	C^α(1)C^β str(18), C^α(2)C^β str(16), CH_3(1) rock 1(10)
1082	C^α(2)C^β str(13), CH_3(2) rock 2(13), C^α(3)C^β str(12)
1078	$C''H_3$ rock 1(52), $C''H_3$ rock 2(21), $C''H_3$ asym bend 1(10)
1070	C^α(3)C^β str(16), C^α(2)C^β str(13)
1049	CH_3(4) rock 1(56), CH_3(4) rock 2(23)
1022	NC'' str(40), CH_3(3) rock 2(29)
1016	CH_3(4) rock 2(43), CH_3(4) rock 1(20)
994	H^α(1) bend 2(44), C^α(1)C^β str(10)

(*continued*)

Frequency (cm^{-1})	Potential Energy Distribution[a]
990	$H^{\alpha}(4)$ bend 2(59), $C^{\alpha}(4)C^{\beta}$ str(12)
984	$H^{\alpha}(3)$ bend 2(31), $H^{\alpha}(2)$ bend 2(18), $CH_3(2)$ rock 1(11)
983	$H^{\alpha}(3)$ bend 2(28), $H^{\alpha}(2)$ bend 2(21), $H^{\alpha}(1)$ bend 2(10)
977	$H^{\alpha}(2)$ bend 2(20), $CH_3(1)$ rock 2(20), $NC^{\alpha}(2)$ str(10)
967	$CH_3(2)$ rock 2(21), $NC^{\alpha}(3)$ str(13), $H^{\alpha}(3)$ bend 2(10)
954	$CH_3(1)$ rock 2(13), $NC^{\alpha}(1)$ str(10)
938	$NC^{\alpha}(4)$ str(22), NC″ str(11), $C^{\alpha}(4)C^{\beta}$ str(11), $CH_3(3)$ rock 2(10)
913	CN(1) str(23), $C'H_3$ rock 1(11), $CNC^{\alpha}(1)$ def(11)
898	CN(4) str(12), $CNC^{\alpha}(4)$ def(11)
897	$C^{\alpha}(1)C$ str(13), CN(2) str(13), C═O(2) str(10)
879	CN(3) str(16)
855	CN(5) str(15), $C^{\alpha}(4)C$ str(14)
762	C═O(2) opb(17), C═O(3) opb(16)
754	C═O(4) opb(13), C═O(5) opb(10)
737	C═O(5) opb(22), C═O(3) opb(14)
721	C═O(4) opb(20), C═O(3) opb(13)
697	C═O(2) ipb(16), C═O(2) opb(13), $C^{\alpha}(1)C$ str(10)
683	C═O(5) ipb(13), C═O(4) opb(11), C═O(5) opb(11)
648	C═O(1) opb(13), $C^{\alpha}(1)CN$ def(12)
645	C═O(5) ipb(11)
633	CN(4) tor(23)
613	C═O(1) opb(40), CN(1) tor(33)
597	C═O(1) ipb(24), CN(4) tor(13), C'C str(10), CN(1) tor(10), CN(3) tor(10)
595	CN(4) tor(30), CN(1) tor(17), CN(2) tor(17), CN(3) tor(12), NH(4) opb(12)
584	CN(1) tor(49), $H^{\alpha}(1)$ bend 2(16), C═O(1) opb(10)
575	CN(3) tor(50), NH(3) opb(23), CN(5) tor(19), NH(5) opb(11)
574	CN(2) tor(44), NH(2) opb(26), NH(5) opb(14), CN(5) tor(13)
570	NH(5) opb(25), CN(2) tor(19), NH(2) opb(12), NH(3) opb(11)
531	C═O(3) ipb(11), C'CN def(10)
500	$NC^{\alpha}(2)C$ def(15), C'CN def(10)
473	H···O(4) str(76)
471	H···O(3) str(80)
469	H···O(1) str(62), H(4)···O(2) str(11)
443	$C^{\beta}(3)$ bend 1(22)
412	C'CN def(22), $C^{\beta}(2)$ bend 1(17)
403	$NC^{\alpha}(3)C$ def(34), $NC^{\alpha}(2)C$ def(10)
370	$C^{\beta}(3)$ bend 2(14), $C^{\beta}(4)$ bend 1(11)
350	$C^{\beta}(2)$ bend 1(21), C═O(2) ipb(11)
332	$C^{\beta}(2)$ bend 2(20), C═O(3) ipb(14)
313	$C^{\beta}(4)$ bend 2(25)
308	$C^{\beta}(1)$ bend 2(18), $NC^{\alpha}(1)C$ def(11)
298	$C^{\beta}(3)$ bend 2(24)
277	CNC″ def(18), C═O(5) ipb(10)
263	$C^{\alpha}(2)C^{\beta}$ tor(13)
257	$C^{\alpha}(4)C^{\beta}$ tor(34), $C^{\alpha}(3)^{\beta}$ tor(11), CNC″ def(10), $C^{\beta}(2)$ bend 2(10)
250	$C^{\alpha}(2)C^{\beta}$ tor(44), $C^{\alpha}(1)C^{\beta}$ tor(21), $C^{\alpha}(3)C^{\beta}$ tor(17)
249	$C^{\alpha}(3)C^{\beta}$ tor(56), $C^{\alpha}(1)C^{\beta}$ tor(29)

(*continued*)

Frequency (cm^{-1})	Potential Energy Distribution[a]
243	$C^{\alpha}(2)C^{\beta}$ tor(32), $C^{\alpha}(1)C^{\beta}$ tor(23), $C^{\alpha}(4)C^{\beta}$ tor(11)
234	$C^{\alpha}(4)C^{\beta}$ tor(30), CNC″ def(16), $C^{\alpha}(4)$CN def(10)
214	$C^{\beta}(1)$ bend 1(15)
206	$C^{\beta}(3)$ bend 1(9)
196	NH(5) opb(11), $CNC^{\alpha}(3)$ def(10)
177	$CNC^{\alpha}(1)$ def(25), $CNC^{\alpha}(2)$ def(11)
163	NH(5) opb(38), C═O(5) opb(12)
153	$CNC^{\alpha}(3)$ def(20), $C^{\alpha}(2)$CN def(14), C′C tor(12)
148	C′C tor(83)
145	NC″ tor(85), NH(5) opb(14)
135	NH(1) opb(21), $CNC^{\alpha}(2)$ def(14), $NC^{\alpha}(1)$C def(12)
131	H(4)···O(2) str(22), NH(1) opb(13)
126	H(5)···O str(46), H(3)···O str(20)
125	H(3)···O str(41),H(2)···O str(30)
123	H(4)···O(2) str(33), NH(3) opb(26)
111	H(4)···O(2) str(28)
92	H(1)···O(5) str(44)
75	NH(4) opb(22), $C^{\beta}(4)$ bend 1(15)
70	H(1)···O(5) str(19), $C^{\beta}(1)$ bend 1(13)
65	C═O(1)···H def(50), $C^{\alpha}(1)$C tor(15)
63	C═O(5)···H(1) def(65)
62	C═O(4)···H def(50), C═O(2)···H(4) def(30)
62	NH(2) opb(15), $C^{\alpha}(2)$C tor(11)
53	$NC^{\alpha}(4)$ tor(21), $C^{\alpha}(3)$C tor(20), NH(4) opb(10), NH(2) tor(10)
39	$NC^{\alpha}(1)$ tor(43)
34	NH(4)···O(2) def(60), NH(3)···O def(10)
33	NH(1)···O(5) def(70), NH(3)···O def(10)
33	NH(5)···O def(70)
31	$C^{\alpha}(2)$C tor(28), NH(1)···O(5) def(13), $NC^{\alpha}(3)$ tor(13)
28	$C^{\alpha}(4)$C tor(60)
25	$C^{\alpha}(1)$C tor(19), NH(4)···O(2) def(12), $NC^{\alpha}(1)$ tor(10)
20	$C^{\alpha}(1)$C tor(25), C═O(5)···H(1) def(14), $NC^{\alpha}(1)$ tor(14), NH(2) opb(10)
20	C═O(3) tor(61), C═O(1) tor(14)
19	C═O(4) tor(60), C═O(2) tor(10)
18	$C^{\alpha}(1)$C tor(33), $C^{\alpha}(2)$C tor(26)
15	$NC^{\alpha}(3)$ tor(27), $C^{\alpha}(3)$C tor(17), $C^{\alpha}(2)$C tor(12), $NC^{\alpha}(4)$ tor(10)
14	NH(4) tor(36), NH(2) tor(14)
13	NH(5) tor(46), NH(1) tor(10)
13	NH(3) tor(47), NH(4) tor(13)

[a] Only contributions equal to or greater than 10% are included. Abbreviations used: asym, asymmetric; def, deformation; ipb, in-plane bend; opb, out-of-plane bend; str, stretch; sym, symmetric; tor, torsion.

I and II modes cannot be accounted for satisfactorily without incorporating the effects of transition dipole coupling. The results of doing so for the type I–III turns are shown in Table IV; the amide III modes are included for convenience in making comparisons between these three characteristic amide modes of the β-turns. Results are shown for several values of the effective dipole moment, $\Delta\mu_{eff}$, since the values derived for the β-sheet

TABLE II
Calculated Frequencies of a Type II β-Turn of CH_3-CO-$(Ala)_2$-Gly-Ala-NH-CH_3

Frequency (cm^{-1})	Potential Energy Distribution[a]
3276–3264	NH str: 5 modes
2979–2978	CH_3 asym str: 10 modes
2941	CH_3 sym str: 5 modes
2932	CH_2 asym str(97)
2876–2874	$C^{\alpha}H^{\alpha}$ str: 3 modes
2863	CH_2 sym str(96)
1676	C=O(5) str(64), CN(5) str(12)
1675	C=O(3) str(65), CN(3) str(12)
1674	C=O(2) str(55), C=O(1) str(14)
1671	C=O(1) str(55), C=O(2) str(16)
1665	C=O(4) str(75), C^{α}CN(4) def(12)
1578	NH(5) ipb(32), $C''H_3$ sym bend(26)
1568	NH(4) ipb(21), NH(1) ipb(20)
1567	NH(1) ipb(33), NH(4) ipb(23)
1563	NH(3) ipb(20), CN(3) str(12)
1553	NH(2) ipb(23), CN(2) str(21)
1468–1462	CH_3 asym bend: 10 modes
1457	CH_2 bend (86)
1391	CH_2 wag(76)
1391	H^{α}(3) bend 1(21), H^{α}(2) bend 1(13)
1390–1378	CH_3 sym bend: 5 modes
1377	H^{α}(1) bend 1(26), H^{α}(3) bend 1(10)
1330	NH(1) ipb(28), C'C str(17)
1329	NH(4) ipb(22), C^{α}(3)C str(18)
1303	NH(2) ipb(19), NH(3) ipb(12)
1297	NH(3) ipb(21), NH(2) ipb(13)
1292	NH(5) ipb(37), C^{α}(4)C str(16)
1250	CH_2 twist(73)
1218	NC^{α}(2) str(24), NC^{α}(1) str(15)
1195	NC^{α}(4) str(38), CH_3(2) rock 1(10)
1184	NC^{α}(1) str(19), NC^{α}(3) str(17)
1153	NC^{α}(2) str(19), NC^{α}(1) str(11)
1127	CH_3(2) rock 1(13), H^{α}(3) bend 2(10)
1110	$C'H_3$ rock 1(33), CH_3(1) rock 2(11)
1107	NC'' str(12), $C''H_3$ rock 2(10)
1106	CH_3(1) rock 1(28), C^{α}(2)C^{β} str(11)
1102	CH_3(2) rock 1(13), CH_3(1) rock 2(13)
1096	C^{α}(1)C^{β} str(25), $C'H_3$ rock 2(13)
1084	$C''H_3$ rock 1(56), $C''H_3$ rock 2(22)
1079	CH_3(4) rock 1(56), CH_3(4) rock 2(22)
1063	C^{α}(4)C^{β} str(20), C^{α}(2)C^{β} str(19)
1049	NC^{α}(3) str(37), CH_3(2) rock 1(16)
1022	NC'' str(40), CH_3(1) rock 1(11)
1016	CH_3(4) rock 2(43), CH_3(4) rock 1(19)
1007	CH_2 rock(50), C=O(4) str(12)
994	H^{α}(1) bend 2(51), C^{α}(1)C^{β} str(11)
990	H^{α}(4) bend 2(58), C^{α}(4)C^{β} str(11)
981	CH_3(2) rock 2(11), CH_3(1) rock 2(10)

(continued)

Frequency (cm^{-1})	Potential Energy Distribution[a]
976	H^{α}(2) bend 2(50), $C^{\alpha}(2)C^{\beta}$ str(14)
944	NC^{α}(2) str(12), CH_3(1) rock 2(10)
935	NC^{α}(4) str(15)
913	CN(1) str(23), CNC^{α}(1) def(11)
895	C^{α}(1)C str(13), CN(2) str(10)
890	CNC^{α}(4) def(8)
883	CN(3) str(14), C^{α}(2)C str(12)
850	CN(5) str(13), C^{α}(4)C str(11)
768	C=O(2) opb(14), CN(2) tor(11)
747	C=O(5) opb(16), C=O(4) opb(12)
734	C=O(5) opb(16), C=O(3) opb(11)
724	C=O(3) opb(31), C=O(4) opb(12)
715	C=O(4) opb(12), C=O(3) ipb(11)
684	C=O(2) opb(17), C=O(2) ipb(10)
674	C=O(5) ipb(17), C=O(5) opb(15)
644	NH(4) opb(20), CN(4) tor(20), CH_2 rock(13)
643	C=O(1) opb(17), C^{α}(1)CN def(11), CH_2 wag(10)
619	CN(1) tor(57), C=O(1) opb(24)
607	CN(1) tor(38), NH(1) opb(29)
600	C=O(1) ipb(21), CN(3) tor(14), CH_2 rock(13)
594	CN(4) tor(46), NH(4) opb(19)
588	CN(3) tor(44), NH(3) opb(40)
572	CN(5) tor(85), NH(5) opb(13)
571	CN(2) tor(59), NH(2) opb(39)
544	C'CN def(17), C=O(1) ipb(11)
481	C^{α}(4)CN def(10)
477	H···O(4) str(62), H(4)···O(2) str(12)
473	H···O(1) str(51), H(1)···O(5) str(10)
472	H···O(3) str(81)
434	C^{β}(2) bend 2(13), C'CN def(11)
424	NC^{α}(3)C def(16)
410	C^{β}(1) bend 1(17), C'CN def(13)
342	C=O(2) ipb(10), CNC^{α}(2) def(10)
318	C^{β}(1) bend 2(27), NC^{α}(2)C def(19)
312	C^{β}(4) bend 2(27), NC^{α}(4) def(14)
287	NC^{α}(1)C def(11), NC^{α}(2)C def(10)
280	C^{β}(2) bend 2(22), C^{β}(2) bend 1(10)
261	$C^{\alpha}(4)C^{\beta}$ tor(24), CNC″ def(19)
256	$C^{\alpha}(1)C^{\beta}$ tor(26), C^{β}(2) bend 1(15)
247	$C^{\alpha}(2)C^{\beta}$ tor(58), $C^{\alpha}(4)C^{\beta}$ tor(12)
241	$C^{\alpha}(1)C^{\beta}$ tor(40)
237	$C^{\alpha}(4)C^{\beta}$ tor(37), $C^{\alpha}(2)C^{\beta}$ tor(12)
220	C^{β}(1) bend 1(13)
209	NH(5) opb(20), C^{β}(4) bend 1(18)
204	C^{β}(2) bend 1(10)
171	CNC^{α}(1) def(30), NH(2) opb(10)
165	NH(5) opb(47), C=O(5) opb(13)
149	C'C tor(93)
145	NC″ tor(86), NH(5) opb(11)
140	CNC^{α}(3) def(27)
135	NH(1) opb(22), CNC^{α}(2) def(15)

(*continued*)

Frequency (cm^{-1})	Potential Energy Distribution[a]
124	CNC^{α}(3) def(26), NC^{α}(3)C def(10)
117	H(5)···O str(41), H(2)···O str(26)
116	H(3)···O str(33), H(5)···O str(31)
113	H(1)···O(5) str(33), H(3)···O str(23)
106	H(1)···O(5) str(28), NC^{α}(2) tor(10)
85	H(4)···O(2) str(28), NH(4) opb(21)
80	NH(1) opb(10)
69	C═O(1)···H def(47), C^{α}(1)C tor(11)
67	C═O(5)···H(1) def(49), C═O(2)···H(4) def(30)
65	C═O(4)···H def(50), C═O(5)···H(1) def(23)
63	H(1)···O(5) str(15), C^{β}(1) bend 1(13)
61	C^{α}(4)C tor(17), NC^{α}(4) tor(14)
54	NC^{α}(4) tor(12), NH(4) opb(11)
42	C═O(5)···H(1) def(20), C^{α}(4)C tor(14)
36	NC^{α}(3) tor(31), C^{α}(2)C tor(20)
35	NH(4)···O(2) def(41), NH(1)···O(5) def(11)
34	NH(3)···O def(45), NH(2)···O def(10)
34	NH(5)···O def(70), NH(1)···O(5) def(10)
28	NC^{α}(1) tor(23), C^{α}(1)C tor(15)
27	C^{α}(4)C tor(25), NH(4)···O(2) def(15)
25	C═O(3) tor(67)
24	C═O(2) tor(53), C═O(4) tor(11)
24	C═O(4) tor(60), C═O(1) tor(15)
21	NC^{α}(1) tor(14), C═O(5) tor(10)
17	NH(4) tor(61), NH(5) tor(11)
16	NH(3) tor(37), NH(1) tor(26)
16	NH(2) tor(63)
14	NC^{α}(3) tor(19), NH(4)···O(2) def(12)

[a] Only contributions equal to or greater than 10% are included. Abbreviations used: asym, asymmetric; def, deformation; ipb, in-plane bend; opb, out-of-plane bend; str, stretch; sym, symmetric; tor, torsion.

structures[10,11] (0.37 D for amide I and 0.27 D for amide II) may not be appropriate for β-turns.

Although we have not included the detailed results for the calculations on β-turns of types I′–III′, the normal modes of these structure have been calculated. For purposes of comparison we present in Table V the amide I–III frequencies of these β-turns, the first two modes incorporating the effects of transition dipole coupling.

The complete effects of structural variations are difficult to present in a concise and easily digestible manner. In addition to the standard structures, we have computed the normal modes of seven different type I structures, seven different type II structures, and six different type III structures, and each would require a table such as Table I to list the predicted frequencies. It seems more useful at this stage to concentrate on the structural dependence of the characteristic amide I–III modes. We show these results in Fig. 2 for variations in $(\phi,\psi)_2$ and $(\phi,\psi)_3$ and in Fig. 3 for variations in $(\phi,\psi)_1$ and $(\phi,\psi)_4$. Since much information is contained in these figures, it is important to explain their content in detail.

TABLE III
Calculated Frequencies of a Type III β-Turn of CH_3-CO-$(Ala)_4$-NH-CH_3

Frequency (cm^{-1})	Potential Energy Distribution[a]
3272–3269	NH str: 5 modes
2979–2977	CH_3 asym str: 12 modes
2942–2941	CH_3 sym str: 6 modes
2975–2874	$C^{\alpha}H^{\alpha}$str: 4 modes
1676	C=O(5) str(68), CN(5) str(14)
1674	C=O(2) str(58), C=O(1) str(16), CN(2) str(10)
1671	C=O(1) str(55), C=O(2) str(17)
1667	C=O(3) str(45), C=O(4) str(32)
1665	C=O(4) str(44), C=O(3) str(32)
1578	NH(5) ipb(32), CN(5) str(17), $C''H_3$ sym bend(28)
1563	NH(1) ipb(52), CN(1) str(27)
1550	NH(2) ipb(38), CN(2) str(27), C^{α}(1)C str(15), C=O(2) ipb(12)
1543	NH(4) ipb(48), CN(4) str(32), C=O(4) ipb(11)
1536	NH(3) ipb(44), CN(3) str(33), C^{α}(2)C str(11), C=O ipb(12)
1468–1451	CH_3 asym bend: 12 modes
1380–1374	CH_3 sym bend: 6 modes
1359	H^{α}(4) bend 1(45),NH(5) ipb(14), CH_3(3) sym bend (13)
1359	H^{α}(3) bend 1(39),H^{α}(2) bend 1(16)
1357	H^{α}(2) bend 1(43), H^{α}(3) bend 1(21)
1351	H^{α}(1) bend 1(41), H^{α}(2) bend 1(19)
1321	NH(1) ipb(30), C'C str(17), CN(1) str(15), C=O(1) ipb(13)
1317	NH(4) ipb(20), C^{α}(3)C str(13)
1303	NH(3) ipb(18), C^{α}(2)C str(10)
1291	NH(2) ipb(25), NH(3) ipb(14)
1286	NH(5) ipb(35), C^{α}(4)C str(16), H^{α}(4) bend 1(13), CN(5) str(12)
1212	NC^{α}(2) str(30), NC^{α}(1) str(22)
1194	NC^{α}(4) str(22), NC'' str(22)
1192	NC^{α}(4) str(25), NC'' str(21), CH_3(2) rock 2(12)
1166	CN^{α}(1) str(25), NC^{α}(2) str(14), CH_3(1) rock 2(10)
1116	NC'' str(18), CH_3(3) rock 2(14), C^{α}(4)C^{β} str(10)
1112	CH_3(3) rock 1(17), $C''H_3$ rock 2(17), C^{α}(4)C^{β} str(13)
1111	$C'H_3$ rock 1(32), $C'H_3$ rock 2(11), C^{α}(1)C^{β} str(10)
1106	CH_3(3) rock 1(18), C^{α}(4)C^{β} str(13)
1098	CH_3(1) rock 1(17), CH_3(1) rock 2(15)
1093	C^{α}(3)C^{β} str(26), CH_3(2) rock 2(23), C^{α}(2)C^{β} str(17), CH_3(1) rock 1(12)
1091	C^{α}(2)C^{β} str(14), C^{α}(1)C^{β} str(11), C^{α}(3)C^{β} str(12), CH_3(1) rock 1(10), CH_3(2) rock 1(10)
1084	C^{α}(2)C^{β} str(15), C^{α}(1)C^{β} str(13), CH_3(2) rock 2(11)
1078	$C''H_3$ rock 1(55), $C''H_3$ rock 2(22)
1068	C^{α}(3)C^{β} str(14), C^{α}(2)C^{β} str(12)
1049	CH_3(4) rock 1(56), CH_3(4) rock 2(23)
1023	CH_3(3) rock 1(30), NC'' str(40), C^{α}(4)C^{β} str(10)
1016	CH_3(4) rock 2(43), CH_3(4) rock 1(20)
995	H^{α}(1) bend 2(42)
992	H^{α}(4) bend 2(54), C^{α}(4)C^{β} str(10)
984	H^{α}(2) bend 2(27), H^{α}(3) bend 2(17), H^{α}(1) bend 2(12)
981	H^{α}(3) bend 2(47), CH_3(1) rock 2(10)

(*continued*)

Frequency (cm^{-1})	Potential Energy Distribution[a]
978	H^{α}(2) bend 2(27), CH_3(1) rock 2(17)
972	CH_3(2) rock 2(17), NC^{α}(3) str(10)
956	NC^{α}(1) str(12), CH_3(1) rock 2(11)
943	NC^{α}(4) str(22), NC″ str(12), $C^{\alpha}(4)C^{\beta}$ str(12), CH(3) rock 2(10)
913	CN(1) str(23), CNC^{α}(1) def(11), C′H_3 rock 1(11)
898	CN(2) str(10), C^{α}(1)C str(10)
895	CN(4) str(10)
880	CN(3) str(16)
855	CN(5) str(16), C^{α}(4)C str(14)
764	C═O(3) opb(17), C═O(2) opb(15)
748	C═O(4) opb(18), C═O(5) opb(13)
745	C═O(4) opb(23), C═O(5) opb(11)
737	C═O(3) opb(19), C═O(2) opb(12)
700	C═O(1) opb(15), C═O(2) ipb(14)
677	C═O(4) opb(17), C═O(5) ipb(15)
671	CN(4) tor(30), NH(4) opb(29),H^{α}(4) bend 2(13), C═O(4) opb(10)
650	C^{α}(1)CN def(14), C═O(1) opb(10)
637	C^{α}(2)CN def(12), C═O(3) opb(10)
631	CN(4) tor(16), C^{α}(3)CN def(10), C═O(5) ipb(10)
616	CN(1) tor(49), C═O(1) opb(37)
599	C′C str(11)
589	C═O(1) ipb(28), CN(1) tor(24), NH(4) opb(16), CN(2) tor(13)
577	CN(1) tor(30), NH(1) opb(23), H^{α}(1) bend 2(13), C═O(1) opb(12), C═O(3) ipb(10)
573	CN(2) tor(43), NH(2) opb(22), NH(5) opb(14), CN(5) tor(14)
573	CN(5) tor(36), CN(3) tor(33), NH(5) opb(19), NH(3) opb(18)
534	C′CN def(15), C═O(4) ipb(10)
497	C′CN def(10), C═O(4) ipb(10), NC^{α}(2)C def(10)
473	H···O(1) str(82), H(4)···O(2) str(10)
473	H···O(3) str(80), H···O(1) str(11)
471	H···O(4) str(81)
469	NC^{α}(2)C def(17), NC^{α}(3)C def(15)
411	C′CN def(22), C^{β}(1) bend 1(17)
393	NC^{α}(3)C def(14), C^{β}(4) bend 1(14), C^{α}(4)CN def(11)
355	C^{β}(3) bend 2(14), C^{β}(2) bend 2(13), C^{β}(2) bend 1(10)
348	CNC^{α}(2) def(11), C^{β}(2) bend 1(10)
330	C═O(3) ipb(17), CNC^{α}(3) def(10), C^{β}(2) bend 2(10)
314	C^{β}(4) bend 2(18)
308	C^{β}(1) bend 2(24), C^{β}(4) bend 2(14)
291	C^{β}(3) bend 2(35), CNC″ def(12)
279	CNC″ def(15), C^{β}(4) bend 1(10)
267	$C^{\alpha}(2)C^{\beta}$ tor(15), C^{β}(2) bend 2(10), $C^{\alpha}(1)C^{\beta}$ tor(10)
257	$C^{\alpha}(4)C^{\beta}$ tor(35), $C^{\alpha}(3)C^{\beta}$ tor(26)
250	$C^{\alpha}(2)C^{\beta}$ tor(45), $C^{\alpha}(1)C^{\beta}$ tor(41)
249	$C^{\alpha}(3)C^{\beta}$ tor(52), $C^{\alpha}(4)C^{\beta}$ tor(28)
241	$C^{\alpha}(2)C^{\beta}$ tor(30), $C^{\alpha}(1)C^{\beta}$ tor(27)
232	$C^{\alpha}(4)C^{\beta}$ tor(23), CNC″ def(17), C^{α}(4)CN def(12)
216	C^{β}(1) bend 1(17), C^{β}(3) bend 2(10)
205	CNC″ def(15)
190	C^{β}(3) bend 1(12), NC^{α}(2) def(10)
175	CNC^{α}(1) def(21), NH(5) opb(18), CNC^{α}(2) def(10)

(*continued*)

Frequency (cm^{-1})	Potential Energy Distribution[a]
166	NH(5) opb(38), C=O(5) opb(10), CNC$^{\alpha}$(1) def(10)
151	CNC$^{\alpha}$(3) def(25), NH(3) opb(10), C$^{\alpha}$(2)CN def(10)
148	C′C tor(89)
144	NC″ tor(88), NH(5) opb(12)
134	NH(1) opb(36), CNC$^{\alpha}$(2) def(14), NC$^{\alpha}$(1)C def(11)
123	H(4)···O(2) str(15), NC$^{\alpha}$(4)C def(13)
115	H(1)···O(5) str(46), C$^{\beta}$(1) bend 1(10)
115	H(2)···O str(44), H(3)···O str(41)
114	H(5)···O str(46), H(3)···O str(21)
114	H(4)···O(2) str(32), NH(3) opb(14)
85	H(1)···O(5) str(17), NH(3) opb(14)
82	CN(4) tor(11), C$^{\beta}$(4) bend 1(10)
66	C=O(1)···H def(55), C′C tor(11)
66	C=O(4)···H def(51)
65	C=O(2)···H(4) def(31), C=O(5)···H(1) def(27)
63	H(4)···O(2) str(24), C$^{\alpha}$(3)C tor(12)
55	C$^{\alpha}$(2)C tor(15), NC$^{\alpha}$(3) tor(14), H(1)···O(5) str(13)
52	H(1)···O(5) str(17), NC$^{\alpha}$(4) tor(14), C$^{\alpha}$(3)C tor(13)
45	NC$^{\alpha}$(1) tor(21), C$^{\alpha}$(4)C tor(11)
36	C$^{\alpha}$(4)C tor(23), NC$^{\alpha}$(1) tor(15), C=O(2) tor(11)
35	NH(3)···O def(70), NH(4)···O(2) def(14)
33	NH(3)···O def(41), NH(1)···O(5) def(11)
31	NH(5)···O def(72), NH(2)···O def(10)
28	NC$^{\alpha}$(1) tor(16), NH(2) opb(11)
24	C$^{\alpha}$(4)C tor(12), NC$^{\alpha}$(3) tor(10)
22	C=O(1) tor(65), C=O(5) tor(14)
21	C=O(5) tor(67), C=O(1) tor(12)
20	C=O(4) tor(63), C=O(2) tor(11)
19	NC$^{\alpha}$(4) tor(20), C$^{\alpha}$(3)C tor(15), C=O(5)···H(1) def(11), NC$^{\alpha}$(1) tor(10)
17	C$^{\alpha}$(1)C tor(40)
14	NH(3) tor(44), NH(4) tor(14)
14	NH(1) tor(47), NH(2) tor(13)
13	NH(5) tor(47), NH(4) tor(11)

[a] Only contributions equal to or greater than 10% are included. Abbreviations used: asym, asymmetric; def, deformation; ipb, in-plane bend; opb, out-of-plane bend; str, stretch; sym, symmetric; tor, torsion.

Each figure consists of three parts, corresponding to the amide I–III frequencies. In each part the frequencies are given only for the amide modes of the peptide groups in the turn, viz., groups 2–4 of Fig. 1. Each group is represented by a symbol, open if the mode is confined to that group and with an interior slash if it mixes with a similar mode in another group. If the second group is 2, 3, or 4, it will have a similarly oriented slash; the absence of a second similar slash means that there is no significant mixing in the second mode or that the mixing is with other groups. Solid lines connect frequencies for type I β-turns, broken lines connect frequencies for type II β-turns, and dotted lines connect frequencies for type III β-turns (the connecting lines are for ease in reading and do not necessarily give the detailed variation of frequency with angle). In any particular graph only

TABLE IV
Calculated Amide Frequencies I–III with Transition Dipole Coupling Included for β-Turn Types I–III

	Type I				Type II				Type III				
	Frequency (cm^{-1})				Frequency (cm^{-1})				Frequency (cm^{-1})				
	$\Delta\mu_{eff}$ (D)				$\Delta\mu_{eff}$ (D)				$\Delta\mu_{eff}$ (D)				
Group	0.0	0.30	0.35	0.45	Group	0.0	0.30	0.35	0.45	Group	0.0	0.30	0.35	0.45
Amide I														
5	1676	1678	1679	1680	5	1676	1680	1683	1686	5	1676	1679	1682	1684
2 + 1	1673	1659	1650	1642	3	1675	1666	1661	1656	2 + 1	1674	1661	1649	1643
1 + 2	1671	1685	1694	1702	2 + 1	1674	1671	1669	1666	1 + 2	1671	1680	1687	1694
3 + 4	1666	1675	1681	1690	1 + 2	1671	1681	1689	1693	3 + 4	1667	1675	1680	1686
4 + 3	1665	1654	1647	1640	4	1665	1661	1659	1657	4 + 3	1665	1657	1652	1648
	0.0	0.20	0.27	0.40		0.0	0.20	0.27	0.40		0.0	0.20	0.27	0.40
Amide II														
5	1579	1575	1568	1559	5	1578	1573	1561	1555	5	1578	1569	1561	1553
4	1569	1561	1555	1536	4 + 1	1568	1564	1557	1547	1	1563	1562	1560	1558
1	1567	1563	1557	1547	1 + 4	1567	1561	1555	1548	2	1550	1554	1559	1562
2	1554	1562	1567	1575	3	1563	1561	1560	1558	4	1543	1545	1549	1551
3	1540	1543	1550	1558	2	1553	1550	1545	1540	3	1536	1536	1537	1539
Amide III														
1		1331			1		1330			1		1321		
4		1324			4		1329			4		1317		
3		1305			2 + 3		1303			3		1303		
2		1299			3 + 2		1297			2 + 3		1291		
5		1293			5		1293			5		1286		

TABLE V
Calculated Amide Frequencies I–III with Transition Dipole Coupling Included for β-Turn Types I′–III′

	Type I′				Type II′					Type III′				
	Frequency (cm^{-1})					Frequency (cm^{-1})					Frequency (cm^{-1})			
	$\Delta\mu_{eff}$ (D)					$\Delta\mu_{eff}$ (D)					$\Delta\mu_{eff}$ (D)			
Group	0.0	0.30	0.35	0.45	Group	0.0	0.30	0.35	0.45	Group	0.0	0.30	0.35	0.45
Amide I														
5	1676	1676	1676	1676	2 + 5	1676	1682	1685	1687	5	1676	1677	1677	1679
2	1675	1677	1678	1680	5 + 2	1676	1674	1673	1673	2	1675	1671	1669	1667
1	1672	1671	1670	1669	1	1673	1673	1673	1673	1	1671	1678	1685	1691
3 + 4	1669	1676	1680	1684	3	1672	1670	1668	1666	3	1669	1674	1676	1678
4 + 3	1685	1657	1651	1646	4	1666	1665	1665	1664	4	1666	1658	1654	1649
	0.0	0.20	0.27	0.40		0.0	0.20	0.27	0.40		0.0	0.20	0.27	0.40
Amide II														
5	1568	1563	1553	1546	5	1569	1565	1559	1551	5	1566	1551	1543	1531
1	1555	1549	1543	1536	1 + 2	1553	1548	1546	1541	1	1555	1552	1550	1549
4	1548	1531	1529	1521	4	1548	1539	1531	1526	4	1546	1549	1552	1553
3	1541	1545	1550	1553	1 + 2	1536	1530	1523	1517	2	1542	1545	1548	1548
2	1536	1538	1542	1544	3	1525	1524	1523	1523	3	1537	1535	1534	1532
mide III														
1		1318			1		1311			1		1311		
4		1311			4		1309			4		1303		
3 + 2		1290			2 + 4		1300			2 + 4		1288		
2 + 3		1273			3 + 2		1273			2 + 3		1274		
5		1268			5		1267			5		1271		

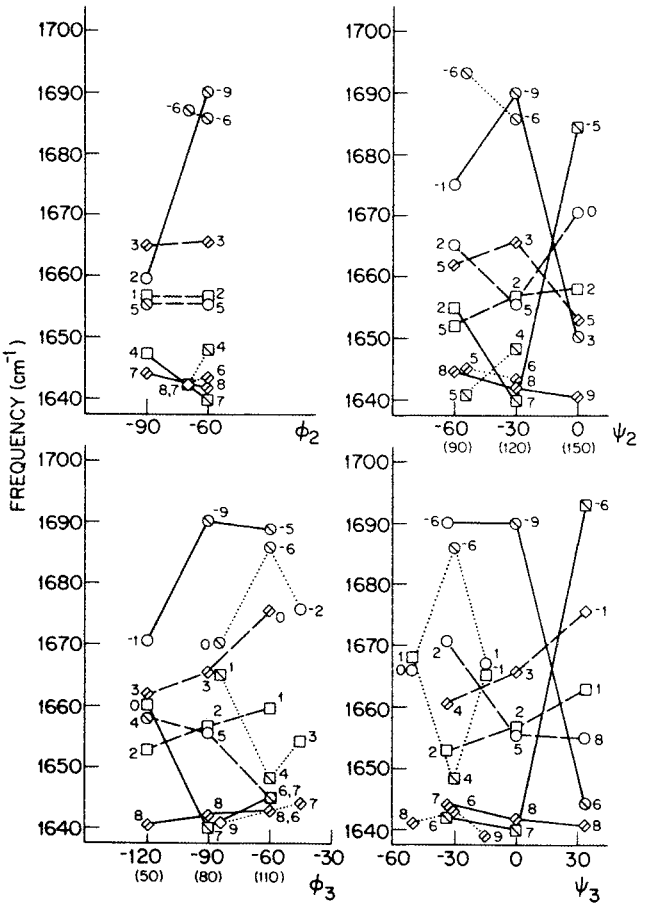

(a)

Fig. 2. Variation of frequency with $(\phi,\psi)_2$ and $(\phi,\psi)_3$ for (a) amide I, (b) amide II, and (c) amide III modes of types I (—), II (- - -), and III (···) β-turns. Symbols indicate peptide group: ◇, 2; ○, 3; □, 4. See text for further details.

the denoted angle is varied; the other angles are kept constant at their standard values. The symbols represent the frequencies for the largest values of $\Delta\mu_{\text{eff}}$, viz., 0.45 D for amide I and 0.40 D for amide II. In order to provide some indication of the effect of change in $\Delta\mu_{\text{eff}}$, we have placed a number next to each symbol to indicate the change in that frequency when $\Delta\mu_{\text{eff}}$ is given the next lowest value that we used, viz., 0.35 D for amide I and 0.27 D for amide II. When two numbers refer to the same symbol (or symbols) it means that two frequencies overlap; in that case the first number refers to the mode of the lower-numbered β-turn (or lower-numbered peptide group).

One other structural variation was considered, viz., a type II β-turn

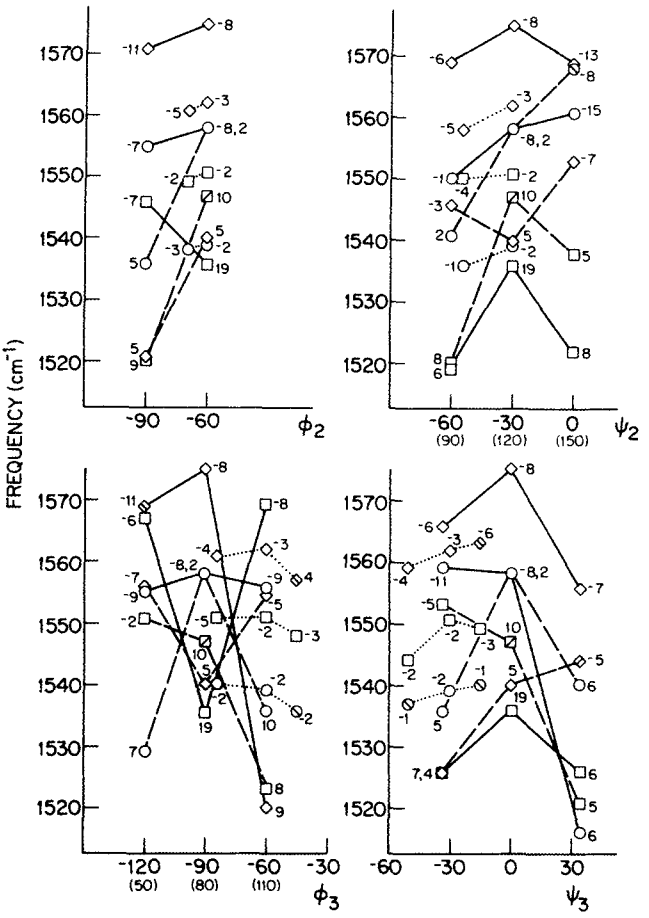

(b)

Fig. 2. (*continued from the previous page*)

without Gly in the third position, over a dozen of which are found in proteins.[5] Of course, the standard dihedral angles are not stereochemically feasible in this case. For this calculation we adopted values of $(\phi,\psi)_2 = -72°, 119°$ and $(\phi,\psi)_3 = 77°, 16°$, which represent the average values of these angles that we obtained from the Protein Data Bank structures. The normal modes were computed for a type II CH_3-CO-$(Ala)_4$-NH-CH_3 with the above angles and $(\phi,\psi)_1 = (\phi,\psi)_4 = -139°, 135°$. The amide I–III frequencies are given in Table VI as a function of $\Delta\mu_{eff}$.

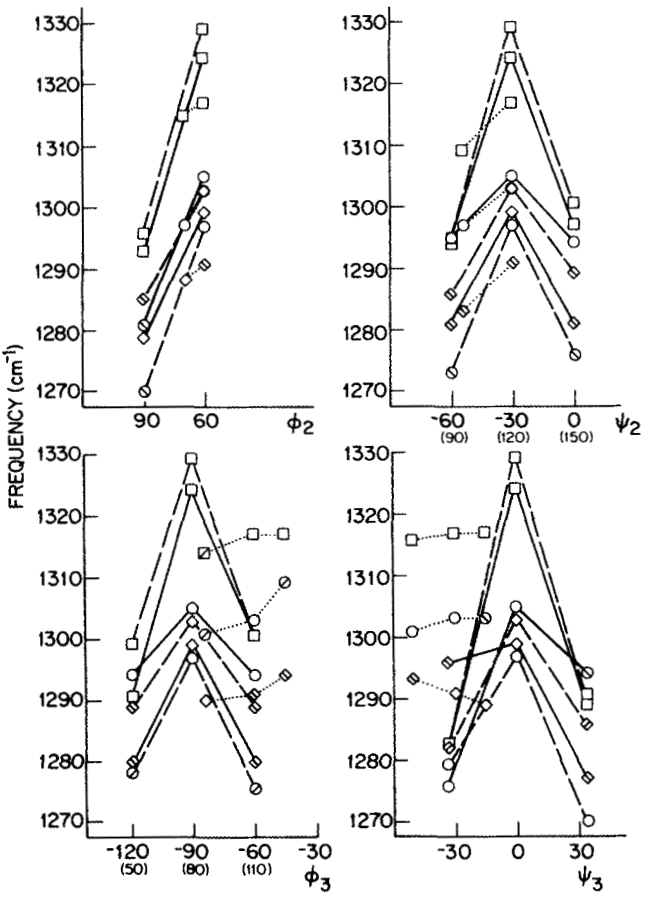

(c)

Fig. 2. (*continued from the previous page*)

DISCUSSION

Standard β-Turns

Several general features of the vibrational spectra of β-turns emerge from these calculations of the normal vibration frequencies. We will consider these here, deferring to later papers the specific assignments associated with particular β-turn structures. In what follows it should be kept in mind that the calculated frequencies cannot be expected to reproduce exactly the observed frequencies; our previous experience[10-12] indicates that discrepancies of at least a few cm^{-1} would not be unusual. We discuss first the frequencies calculated for the characteristic amide modes, both for the β-turn structures as well as for the α-helix and the antiparallel-chain

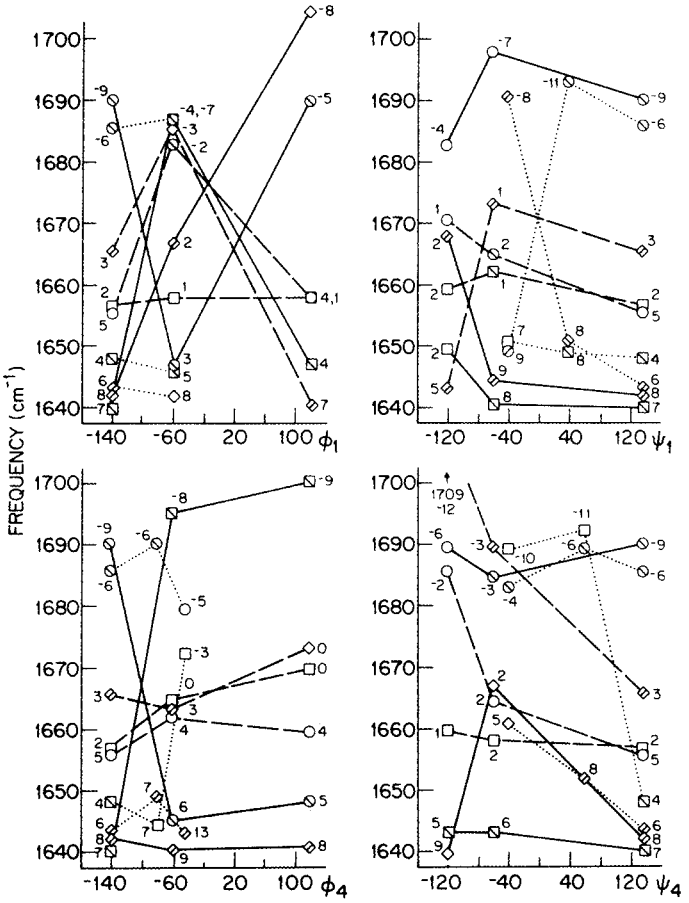

(a)

Fig. 3. Variation of frequency with $(\phi,\psi)_1$ and $(\phi,\psi)_4$ for (a) amide I, (b) amide II, and (c) amide III modes of types I (—), II (- - -), and III (···) β-turns. Symbols indicate peptide group: ◇, 2; ○, 3; □, 4. See text for further details.

pleated sheet, $\beta(\#)$. These results are collected in Table VII for groups 2–4 in the turn.

With respect to the amide I modes, the frequencies associated with groups in the type II β-turn differ significantly from those predicted for types I and III. If we look only at the frequency ranges into which the modes fall for groups 2–4 (without regard to the group involved), then for the type I β-turn we expect frequencies near 1640 and 1690 cm^{-1}; for the type II β-turn the comparable regions are about 1656 and 1666 cm^{-1}; and for the type III β-turn these are 1646 ± 3 and 1686 cm^{-1}. (These figures are applicable for $\Delta\mu_{eff}$ = 0.45 D. For $\Delta\mu_{eff}$ = 0.35 D the numbers are somewhat different, but the same general observations are valid.) It might

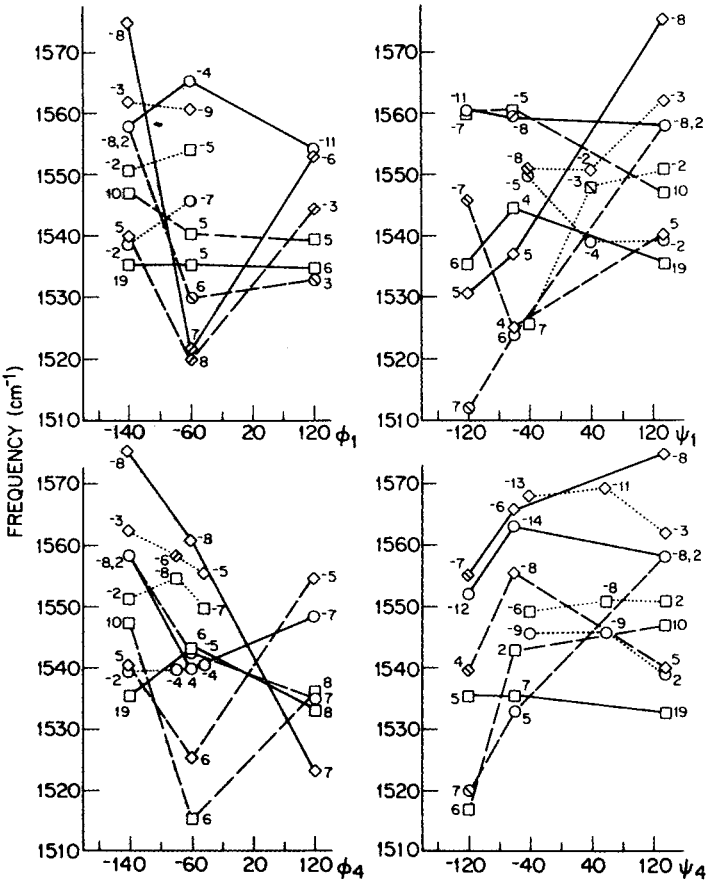

(b)

Fig. 3. (*continued from the previous page*)

be difficult to distinguish between types I and III (although the frequency gap between the ranges is larger for type I, viz., 50 cm^{-1}, than for type III, viz., 40 cm^{-1}), but the frequencies for type II and their gap (10 cm^{-1}) are sufficiently distinct so that this β-turn should be clearly distinguishable from the others. (At this stage we leave out consideration of types I′–III′, since they are found so much less frequently.)

In order to identify β-turns in the presence of other structures that occur in proteins and polypeptides, such as β-sheets and α-helices, it is important to know whether the frequencies given above overlap those of the latter structures. For β-poly(L-alanine) our calculations[11] predict the following amide I frequencies (which have observed counterparts): 1695 cm^{-1} (ir, $\parallel$), 1669 cm^{-1} (Raman), and 1630 cm^{-1} (ir, $\perp$). For α-poly(L-alanine) our calculations[12] predict the following (observed) amide I frequency: 1659

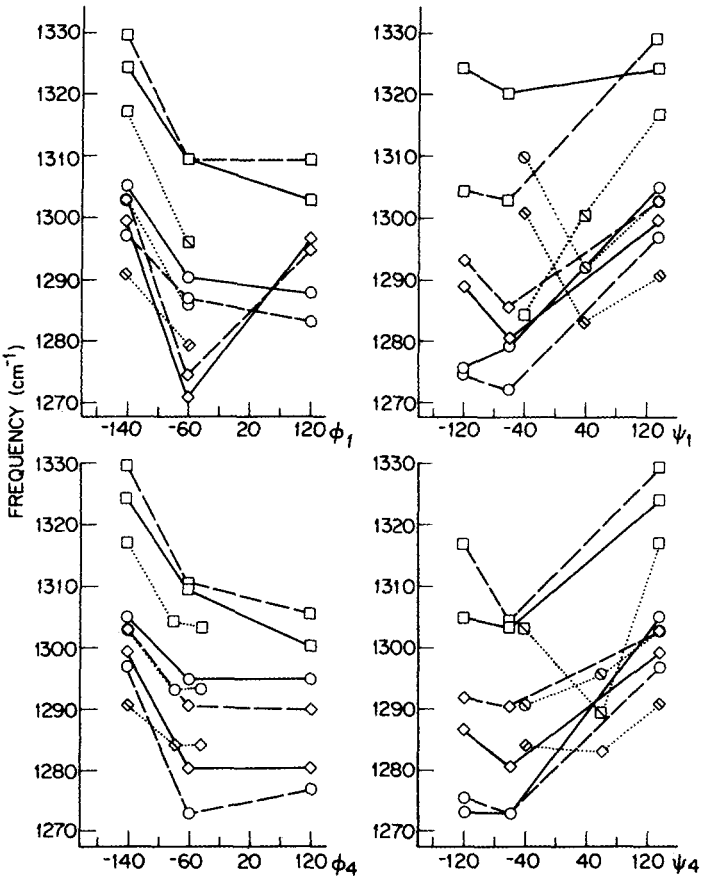

(c)

Fig. 3. (*continued from the previous page*)

cm^{-1} (Raman and ir, ||). Since β-turns lack symmetry, we would expect all of their normal modes to be potentially active in ir and Raman spectra. Allowing for the fact that observed bands for these structures cover a range of values,[14] it seems reasonable to associate a range of $\pm$ 5 cm^{-1} with the β-sheet and α-helix frequencies. Thus the 1640-cm^{-1} band of the type I β-turn comes close to overlapping one band of the β-sheet, whereas the 1690 cm^{-1} band is essentially coincident with a β-sheet frequency. As we have already noted,[1] this therefore means that the presence of a band near 1690 cm^{-1} in the ir spectrum of a protein should not be taken as a unique indication of the presence of antiparallel-chain pleated-β-sheet structure. For type II β-turns the predicted band at 1656 cm^{-1} overlaps the strong band of the α-helix, whereas the 1666-cm^{-1} band overlaps the Raman band of the β-sheet. Of course, in the latter case the β-turn would not exhibit ir

TABLE VI
Calculated Frequencies with Transition Dipole Coupling Included for a Type II β-Turn of CH_3-CO-$(Ala)_4$-NH-CH_3

	Frequency (cm^{-1})			
	$\Delta\mu_{eff}$			
Group	0.0	0.30	0.35	0.45
Amide I				
5 + 3	1676	1676	1677	1679
3 + 5	1676	1665	1658	1653
2 + 1	1673	1672	1672	1671
1 + 2	1671	1685	1694	1702
4	1665	1662	1659	1659
	0.0	0.20	0.27	0.40
Amide II				
5	1566	1563	1556	1551
4 + 3	1553	1548	1541	1536
1	1551	1548	1540	1533
4	1546	1541	1536	1531
2	1534	1530	1527	1523
Amide III				
1		1311		
4		1302		
2 + 3		1284		
3 + 2		1274		
5		1271		

bands near 1630 and 1690 cm^{-1}. The frequencies of the type III β-turn would overlap less with those of the β-sheet than was the case for the type I β-turn, but the coincidences are close. Our calculations thus clearly indicate that caution is necessary in using the traditional frequency assignments of amide I bands in proteins, and especially in the interpretation of intensity changes in terms only of changes in α-helix and β-sheet content. The situation is, of course, helped by obtaining both ir and Raman spectra, since, as can be seen from Table VII, various mutually exclusive assignments are possible.

The amide II modes of the β-turns seem to span fairly uniformly the range of about 1536–1562 cm^{-1}, the type I β-turn being the only one with a distinctively high frequency of 1575 cm^{-1}. The predicted (and observed) modes of the regular structures are somewhat lower: 1523–1555 cm^{-1} for the β-sheet[11] and 1520–1543 cm^{-1} for the α-helix.[12] Therefore, it may be possible to infer the presence of type I β-turns from an analysis of the amide II region.

All of the amide III modes of the β-turn types I–III are predicted in the region of 1290–1330 cm^{-1}, and these β-turns are probably not distinguishable from one another. What is interesting, however, is that this range is at a significantly higher frequency than those associated with β-sheet and α-helix structures, thus providing a possibility for a diagnostic for β-turns. For β-poly(L-alanine) the calculated amide III modes occur in

TABLE VII
Calculated Amide Mode Frequencies for Various Structures

Mode	Structure				
	α[a]	β(ill)[b]	β_I	β_{II}	β_{III}
Amide I		[1701][c]			
		1695	1690		1686
	[1663]	1669		1666	
	1659			~1656	
	[1650]	1630	~1640		1646 ± 3
Amide II		[1587]	1575		
	[1546]	1555	1558	1558	1562
	1543			1547	1551
		1534	1536	1540	1539
	1520	1523			
Amide III			1324	1329	1317
			1305	1303	1303
	1287		1299	1297	1291
	1270				
		1247			
		1228			
		1225			
Amide V	639]	[709]	595	644	671
	628	713	575	607	589
	609	702	574	594	577
	[559]	[699]	570	588	573
				572	573
				571	

[a] From Ref. 12.
[b] From Ref. 11.
[c] Not observed.

the 1225–1247-cm^{-1} region[11] and are usually associated with strong Raman bands observed at frequencies no higher than 1240 cm^{-1}.[14] For α-poly-(L-alanine) the calculated modes are found in the 1270–1287-cm^{-1} region[12] but give rise to relatively weak ir and Raman bands (either because the NH ipb contribution is so low—about 10%—or because CN str makes very little contribution). It is therefore possible that bands associated with β-turns can be observed in the region near and above 1300 cm^{-1}.

Of course, it must be remembered that the amide III mode is sensitive to side-chain composition and to backbone conformation,[14] and it therefore must be used with caution in characterizing peptide structure. In the above examples of poly(L-alanine), this mode has significantly different character in the two structures. In β-poly(L-alanine), bands are observed at ~1222 and 1242 cm^{-1}, which have the usual amide III character: NH ipb(17) + CN str(14) in the first case and NH ipb(19) + CN str(18) in the second. The observed Raman band at 1368 cm^{-1} is mainly H$^{\alpha}$ bend(22), C$^{\alpha}$C str(17), and CH_3 sym bend(13), but it also includes an NH ipb(20) contribution. On the other hand, in α-poly(L-alanine) no band in this region exhibits the typical amide III character, viz., NH ipb + CN str: CN str does

not appear at the 10%, or above, level, and NH ipb contributes at this level to five bands in the 1270–1346-cm^{-1} region. The situation for the β-turns exhibits similar differences (cf. Tables I–III). For the type I β-turn the frequencies associated with the turn (1324, 1305, and 1299 cm^{-1}) all involve NH ipb + CN str. For the type II β-turn, CN str contributes to none of the three modes, which involve only NH ipb (and some CC str), although NH(2) ipb and NH(3) ipb mix for two of these. For the type III β-turn there is again no CN str contribution, and only one mode shows a significant admixture of two NH ipb contributions. A study of actual structures will be necessary to reveal the characteristic intensities associated with these modes (and, in fact, whether transition dipole coupling must be included to explain amide III frequencies).

The amide V modes, associated with NH opb coordinates, have been shown[15] to be particularly sensitive to conformation: they are assigned to bands in the 610–620 cm^{-1} region for α-helical structures and in the 700–705-cm^{-1} region for β-sheet structures.[16] These assignments are supported by detailed normal vibration calculations,[11,12] which also show that other internal coordinates make varying contributions to the bands observed for these structures. What is particularly interesting is that although the frequency regions associated with the β-turns overlap, they are in general lower than the observed bands for the α-helix: 570–575 and 595 cm^{-1} for type I, 571–607 and 644 cm^{-1} for type II, and 573–589 and 671 cm^{-1} for type III (see Table VII). The highest frequency for each type of β-turn is distinctive for that turn, and may be a diagnostic for the structure. Of course, these frequency predictions say nothing regarding relative intensities expected for observed bands; these will have to await an analysis of actual structures. Nevertheless, our calculations suggest that the amide V modes may be useful in identifying the presence of β-turns, and perhaps even in distinguishing between various types.

The amide VI modes, associated with C=O opb coordinates, were originally[15] thought to be characteristically observed near 600 cm^{-1}, but detailed calculations indicate that they are very sensitive to side-chain structure and main-chain conformation. In polyglycine I[10] the main amide VI modes are calculated in the frequency range of 585–618 cm^{-1}, with corresponding bands being observed at 589 (ir and Raman) and 614 (ir) cm^{-1}. In β-poly(L-alanine)[11] these modes shift up to the 682–703-cm^{-1} region, the only assignable band being a Raman band at 698 cm^{-1}. And in α-poly(L-alanine)[12] the main amide VI modes are calculated in the region of 701–782 cm^{-1}, with observed bands being found at 692 (ir and Raman), 756 (Raman), and 774 (ir and Raman) cm^{-1}. Thus in known regular conformations, amide VI modes span a range of almost 200 cm^{-1}. For the β-turns we calculate the following ranges for the main amide VI modes: type I, 721–762 cm^{-1}; type II, 724–747 cm^{-1}; type III, 737–764 cm^{-1}. Since these ranges significantly overlap that of the α-helix (and for a type I β-turn possibly that of the β-sheet), and since amide VI modes (in distinction to amide V) tend to be weak bands, it seems that these modes will be less

useful in identifying β-turns than those listed in Table VII. Again, however, more definitive assessments must await detailed experimental studies of β-turn structures.

We have made only a cursory examination of the low-frequency region for the β-turn structures, even though this region might be expected to be quite sensitive to backbone conformation. The various modes in this region have frequencies that are generally within about 10 cm^{-1} of one another, so that a distinction between different types of β-turns does not seem to be feasible. The composition of these modes does, however, differ from one β-turn to another, and this may give rise to characteristic intensity differences between different structures. Again, a detailed understanding will probably have to await a study of some known structures.

Structural Variations

The most general statement that can be made about the effects of variations in structure of β-turns on their characteristic amide frequencies is that changes in conformation cause these frequencies to shift, usually by significant amounts. The origins of these shifts differ for the different modes; we will consider first the reasons for this.

In the case of amide I, the shifts in frequency with structure arise primarily from the effects of variation in transition dipole coupling. As can be seen by comparing Tables I–III, the amide I frequencies of β-turn types I–III are essentially the same in the absence of transition dipole coupling. Nor are these frequencies affected much by varying the ϕ, ψ over the range we have considered (although it should be noted that the mixing between different group modes does change with variation in the torsion angles). It is only when transition dipole coupling is included, with its explicit dependence on the separation and relative orientation of the C=O stretching transition moments,[8,9] that large frequency splittings result which vary sensitively with the structural parameters. This is, of course, a consequence of the significant coupling that is introduced between amide I vibrations of adjacent peptide groups. As can be seen from Figs. 2(a) and 3(a), although some modes of the peptide groups in the turn are influenced more than others by a change in a given torsion angle, changes in each of the torsion angles $(\phi,\psi)_1$ to $(\phi,\psi)_4$ affect some of the frequencies. In particular, this is true of ϕ_2 and ψ_3, so that it is not possible to attribute shifts in characteristic amide frequencies to variations in local conformational parameters alone, viz., ψ_2 and ϕ_3 in this case. Nonadjacent torsion angles have a significant influence on the amide I frequencies of a given peptide group.

For the amide II modes the frequency dependence on conformation arises from coupling effects due to the internal force field as well as from transition dipole coupling. As can be seen from Tables I–III, even in the absence of transition dipole coupling, the amide II frequencies of peptide groups 3 and

4 vary significantly between β-turn types I–III: for group 3 the frequencies are similar for types I and III but significantly different for type II, and for group 4 the frequencies are similar for types I and II but significantly different for type III. An analogous variation occurs when the torsion angles are changed, the frequencies of group 2 also being affected in this case. Of course, when transition dipole coupling is included, additional frequency shifts occur, the total changes with angle being given in Figs. 2(b) and 3(b). Again we see that amide II frequencies are influenced significantly by the values of nonadjacent torsion angles.

The amide III modes are not perturbed significantly by transition dipole coupling, and the dependence of frequency on conformation in this case arises entirely from internal coupling effects and changes in $H_4 \cdots O_2$ and $H_1 \cdots O_5$ hydrogen bond distances. As can be seen from Figs. 2(c) and 3(c), nonadjacent torsion angles are again influential in affecting the amide III frequency. Incidentally, since all torsion angles have a comparable effect on the amide III frequency, it is not possible to correlate this frequency with ψ_2 alone, as has been suggested.[17] In fact, as we have pointed out,[1] such a correlation would place β-turn frequencies near 1275 cm^{-1} for types I and III and near 1230 cm^{-1} for type II, whereas our calculations predict these frequencies to be in the 1290–1330-cm^{-1} region (cf. Table IV).

The specific effects of changes in ϕ,ψ on the frequencies of β-turn vibrations, depicted in Figs. 2 and 3, are clearly quite complex. Some angular changes produce large, and others small, frequency shifts, and these vary with the type of β-turn. The changes shown in Figs. 2 and 3 are due to single angle changes; the effect of altering two angles simultaneously has not yet been explored in detail. At this stage it is, therefore, probably more useful to use these results only as a general indication of how conformational changes can influence the frequencies, leaving specific predictions to the cases of actual structures.

For the case of a type II β-turn with alanine in the third position, whose (ϕ,ψ) differ slightly from those of the standard type II turn, it is interesting to observe that significant frequency shifts occur. In the first place, it will be seen (cf. Tables IV and VI) that the amide II and III modes of the alanyl structure are predicted at frequencies of ~15–25 cm^{-1} lower than those of the glycyl structure, despite the fact that the amide I frequencies are within a few cm^{-1} of each other. Moreover, the values of the amide II and III frequencies are close to those of the α-helix, thus indicating that overlap for these structures is highly probable in these regions. The amide V modes of the alanyl type II β-turn are predicted at 648, 602, 587, 572, and 570 cm^{-1}, frequencies which are not significantly different from those of the glycyl type II β-turn. It would thus seem that the alanyl type II β-turn is distinguishable from other β-turns by its low amide II and III frequencies, but it may be difficult to distinguish from the α-helix unless its amide V mode shows up at a lower frequency.

CONCLUSIONS

The calculations of the normal vibrations of β-turns provide important insights into the characteristic frequencies of these structures. In particular, they show that some of the modes have frequencies that overlap with those of the main regular structures, viz., the α-helix and the β(‖)-sheet. To the extent that this occurs, it is clear that a more sophisticated interpretation of the vibrational spectra of proteins will be necessary if reliable structural assignments are to be made. On the other hand, some β-turn frequencies are characteristic of these structures, thus providing the possibility of identifying their presence from the ir and Raman spectra.

Another important conclusion of the present work is that the amide III modes of β-turns generally occur at frequencies significantly higher (viz., $\sim$1300–1330 cm^{-1}) than those of α-helix and β-sheet structures. This prediction is supported by recent studies[18] on a type I β-turn tetrapeptide of known structure, in which a strong ir band observed at 1294 cm^{-1} (and calculated at 1291 cm^{-1}) is found to disappear on deuteration. It should be noted that the general frequency region in which the amide III modes are expected will depend sensitively on the nature of the external and internal hydrogen bonding. We have already seen[1] that in the absence of external hydrogen bonds, the amide III frequencies are $\sim$20 cm^{-1} lower. The present structure variation studies show that when internal hydrogen bonds are weakened (which occurs since the H···O distances are increased by most changes in ϕ or ψ), the amide III frequencies are also decreased. It is thus possible that the lower-frequency bands (1266–1278 cm^{-1}) recently found in the Raman spectra of oxytocin and its analogs[19] and related hormones,[20] and which have been assigned to amide III modes of postulated β-turns in these molecules, are a result of weaker hydrogen bonds associated with these conformations.

In subsequent papers on this subject we will deal with assignments for β-turns in specific structures. Because the ϕ,ψ in these may be slightly different from the "standard" values, their frequencies may vary somewhat from those presented here. The present calculations, however, provide a basis for general assignments of β-turn structures in peptides and proteins in that they indicate the key frequency regions to be looked at.

This research was supported by National Science Foundation Grants PCM76-83047 and CHE78-00753. One of us (J.B.) wishes to acknowledge support from a postdoctoral fellowship from the Macromolecular Research Center.

References

1. Bandekar, J. & Krimm, S. (1979) *Proc. Natl. Acad. Sci. USA* **76,** 774–777.
2. Venkatachalam, C. M. (1968) *Biopolymers* **6,** 1425–1436.
3. Geddes, A. J., Parker, K. D., Atkins, E. D. T. & Beighton, E. (1968) *J. Mol. Biol.* **32,** 343–358.
4. Lewis, P. N., Momany, F. A. & Scheraga, H. A. (1973) *Biochim. Biophys. Acta* **303,** 211–229.
5. Chou, P. Y. & Fasman, G. D. (1977) *J. Mol. Biol.* **115,** 135–175.

6. Shields, J. E., McDowell, S. T., Pavlos, J. & Gray, G. R. (1968) *J. Am. Chem. Soc.* **90,** 3549–3556.
7. Kawai, M. & Fasman, G. (1978) *J. Am. Chem. Soc.* **100,** 3630–3632.
8. Krimm, S. & Abe, Y. (1972) *Proc. Nat. Acad. Sci. USA* **69,** 2788–2792.
9. Moore, W. H. & Krimm, S. (1975) *Proc. Natl. Acad. Sci. USA* **72,** 4933–4935.
10. Moore, W. H. & Krimm, S. (1976) *Biopolymers* **15,** 2439–2464.
11. Moore, W. H. & Krimm, S. (1976) *Biopolymers* **15,** 2465–2483.
12. Rabolt J. F., Moore, W. H. & Krimm, S. (1977) *Macromolecules* **10,** 1065–1074.
13. Moore, W. H. & Krimm, S. (1973) *Spectrochim. Acta, Part A* **29,** 2025–2042.
14. Hsu, S. L., Moore, W. H. & Krimm, S. (1976) *Biopolymers* **15,** 1513–1528.
15. Miyazawa, T. (1967) *Poly-α-Amino Acids,* Fasman, G. D., Ed., Dekker, New York, p. 69.
16 Masuda, Y., Fukushima, K., Fujii, T. & Miyazawa, T. (1969) *Biopolymers* **8,** 91–99.
17. Lord R. C. (1977) *Appl. Spectrosc.* **31,** 187–194.
18. Bandekar, J. & Krimm, S. (1979) Sixth American Peptide Symposium, Washington, D.C., Paper C-37.
19. Hruby, V. J., Deb, K. K., Fox, J., Bjarnason, J. & Tu, A. T. (1978) *J. Biol. Chem.* **253,** 6060–6067.
20. Tu, A. T., Lee, J., Deb, K. K. & Hruby, V. J. (1979) *J. Biol. Chem.* **254,** 3272–3278.

Received April 6, 1979
Accepted August 6, 1979